Malaysian Journal of Chemistry, 2021, Vol. 23(3), 92-107

Potentiometric Determination of Fixed Charge Density and Antibacterial Activity of Barium Molybdate Model Membrane

Afren Ansari[1], A. K. Shukla[1] and Mohd. Ayub Ansari[2*]
[1]Department of Chemistry, S.M.S. Govt. Model Science College, Gwalior-474009, Madhya Pradesh, India
[2]Department of Chemistry, Bipin Bihari College, Jhansi-284001, Uttar Pradesh, India
*Corresponding author (e-mail: drayub67@gmail.com)

A barium molybdate parchment-supported model membrane was prepared by the ion interaction method. The electrochemical properties of the membrane were studied using Teorell-Meyer-Sievers, Kobatake and Nagasawa approaches. These properties were used to determine important membrane parameters like fixed charge density, transport number, mobility ratio and permselectivity. The experimental and theoretical membrane potential values were used to calculate charge density. These membrane potential values were compared with those from different approaches of thermodynamics of irreversible processes. The fixed charge density values of the prepared membrane under different electrolytic environments were found to follow the order: LiCl > NaCl > KCl. The membrane was characterized by different instrumental techniques such as SEM, TEM, FTIR, TGA/DTA, XRD and EDX analysis. The antibacterial activity of the model membrane was also studied against Gram-negative and Gram-positive bacteria using the disc diffusion method.

Key words: Barium molybdate model membrane; membrane potential; fixed charge density; transport properties; permselectivity; antibacterial activity

Received: January 2021; Accepted: April 2021

Membranes have widely been used in food, drugs, wastewater treatment and dairy industries. Model membranes have additionally been used for commercial applications such as electrolysis, electrodeionization, fuel cell technology, energy saving, power generation, etc. [1-4] Membrane electrode potentiometry has become a well-established electrochemical method for the determination of lead in environmental samples. It possesses a lot of advantages such as simple instrumentation, low cost, fast response time and selectivity [5, 6] over various other analytical techniques used for this purpose [7, 8]. In order to evaluate charge density, the investigated membrane should not be affected by extreme pH solutions. The performance of the model membrane is determined by its electrochemical properties and these properties depend on physical parameters such as ion exchange capacity, water uptake, thickness, porosity, transportation etc. [9-12].

The measurement of membrane electrical potential [13] is important to characterize transport processes. Membrane potential is defined as an electrical potential difference arising between salt solutions with various concentrations at a constant temperature and pressure, when they are separated by a uniform charged membrane [14, 15]. The ionic selectivity of the model membrane depends only on its fixed charge density. The membrane's role between the electrodes is that of conduction of produced hydrogen ions from anode to cathode and as a barrier to the crossover of fuel [16, 17]. Inorganic materials such as barium (Ba) are suitable as antibacterial agents to kill bacteria or inhibit its growth as they are effective against a broad spectrum of both Gram-negative and Gram-positive bacteria [18].

This paper describes the preparation of a barium molybdate parchment-supported model membrane. Three different and prominent bacterial cultures i.e., *Escherichia coli*, *Pseudomonas aeruginosa* and *Staphylococcus aureus*, were used to study the antibacterial behavior of this membrane. The experimental and theoretical data of the membrane potential were compared. Thermo-dynamically-effective fixed charge density and various membrane parameters were calculated from the membrane potential measurements using Teorell-Meyiers-Sievers (TMS), Kobatake and Nagasawa approaches based on the thermodynamics of irreversible processes.

MATERIALS AND METHOD

Sodium molybdate (S.D. Fine Limited, India), barium chloride (Ranbaxy, India) and parchment paper (Amol Group of Companies, Mumbai, India) were used to synthesis the model membrane. All other reagents used were analytical grade. The uni-univalent chlorides of sodium, potassium, and lithium salts were used for electrochemical characterization.

Membrane Preparation

The parchment-supported barium molybdate model membrane was synthesized by the method of interaction as described by Beg and coworkers [19-22]. To precipitate these substances in the interstices of parchment paper, a 0.2 molar solution of sodium molybdate was placed inside a glass tube, to one end of which was tied the parchment paper previously soaked in deionized water. The tube was suspended for 72 hours in a 0.2 molar solution of barium chloride. The two fresh solutions were later interchanged and kept for another 72 hours. Thus, the combination of the parchment paper and the inorganic precipitate acts as a model membrane. The membrane thus prepared was washed many times with deionized water to remove free electrolytes.

Measurements of Membrane Potential

The freshly prepared membrane was placed between two half cells. The half cells were first filled with a salt solution (KCl, NaCl or LiCl) to equilibrate the membrane. The salt solution was stirred by means of magnetic stirrers. The electrochemical cell as shown in Figure 1

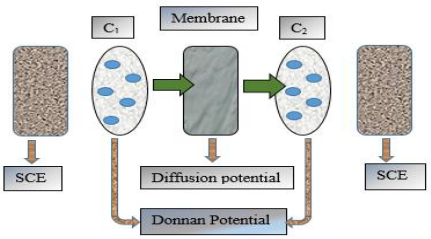

Figure 1. The electrochemical set up for membrane potential measurements

was used for determining the membrane potential passing through the membrane by maintaining a tenfold difference in concentration (C_2/C_1=10). Measurements were made using a multimeter (Rishmulti$^{(R)}$ $4^{3/4}$ digits 18S). All salt solutions used in the investigation were prepared from analytical grade reagents and distilled water [23].

Characterization of Membrane

Membrane parameters such as water uptake, porosity, thickness, swelling etc. influence the electrochemical properties of the membrane, therefore it is necessary to be characterized the complete membrane. These parameters were determined by Arsalan et al. [24].

Water uptake (% total wet weight), Porosity, Thickness, Swelling, SEM, TEM, FT-IR, TGA/DTA, XRD and EDX Studies of the Membrane

The prepared membrane was soaked in deionized water for 2 h, blotted quickly with Whatman filter paper to remove surface moisture and immediately weighed. These were further dried to a constant weight in vacuum over P_2O_5 for 24 h. Porosity was calculated as the volume of water absorbed in the cavities per unit membrane volume from the water uptake data. The thickness of the membrane was determined by measuring the average thickness of the membrane with a screw gauge. The swelling of the membrane was measured as the difference between the average thickness of the dry membrane equilibrated in one molar solution of sodium chloride for 24 h, and the dry membrane. Scanning electron microscopy (SEM) is a type of electron microscopy that produces images of a sample by scanning it with a focused beam of electrons. The characterization, pore structure, micro/macro porosity, homogeneity, thickness, cracks and surface morphology of the barium molybdate model membrane were investigated with an Oxford scanning electron microscope model JSM-7100F. The membrane sample was coated with gold sputter at pressure of 1 Pa. Transmission electron microscopy (TEM) analysis was performed to determine the particle size of the parchment-supported barium molybdate membrane. The TEM image of the membrane was obtained using a Thermo Scientific^{TM} Talos L120C transmission electron microscope. The Fourier-transform infrared (FT-IR) spectrum of the parchment-supported barium molybdate membrane was obtained using a Bruker Tensor 27 spectrophotometer. The entrance and exit beams to the sample compartment were sealed with a coated KBr window and there was a hinged cover to seal it from the surroundings. The degradation process and thermal behavior of the parchment-supported membrane was investigated using thermogravimetric analysis (TGA) under nitrogen atmosphere using a heating rate of 20°C min^{-1} from 25 to 600°C and differential thermal analysis (DTA) using a Toledo-Mettler thermal analyzer. The X-ray diffraction (XRD) pattern of the parchment-supported barium molybdate membrane was recorded with an X-ray diffractometer (Panalytical X^1pert Power) with Cu Kα radiation. The Energy Dispersive X-Ray (EDX) spectra of the model membrane was obtained using a scanning electron microscope (model JSM-7100F Oxford).

Antibacterial Activity of the Membrane

The antibacterial activity of the prepared membrane against three bacterial organisms was tested using the disc diffusion procedure [25, 26]. The organisms used were *Escherichia coli*, *Pseudomonas aeruginosa* and *Staphylococcus aureus*, and proper control was maintained with solvents using nutrient agar plates. Initially, organisms were grown separately in a nutrient broth and incubated overnight at 37°C. After 12 h the bacterial growths in the nutrient broth were poured on the nutrient agar plates and permitted to stand for a minute. The excess cultures were removed

after a while. A well with a diameter of 8 mm was cut in this nutrient agar with the help of microtips (normally utilized with micropipettes of 100 to 1000 mL). One well was cut at an equal distance in each plate. The bottom of the well was sealed with a drop of fresh molten nutrient agar and allowed to stand for some time so that it could harden. Each well was filled with the different preparations and incubated at 30°C for 24 h. After 24 h the plates were observed for the inhibition of bacterial growth indicated by clear zones around the well. The diameter of the clear zones were measured with a ruler and recorded. The test was also performed with different antibiotics against these organisms for as a comparative study.

RESULTS AND DISCUSSION

The results of water uptake, porosity, thickness, and swelling of the barium molybdate parchment-supported membrane are given in Table 1.

Table 1. Water content, porosity, thickness, and swelling properties of barium molybdate model membrane

Water uptake as % weight of wet membrane	1.086
Porosity (Φ)	0.0657
Thickness (cm)	1.055
Swelling (%)	0.99

The water uptake of the model membrane depends on the vapour pressure. A high water uptake, swelling and porosity with a thinner model membrane implies that the diffusion within the membrane occurs mainly through exchange sites [27].

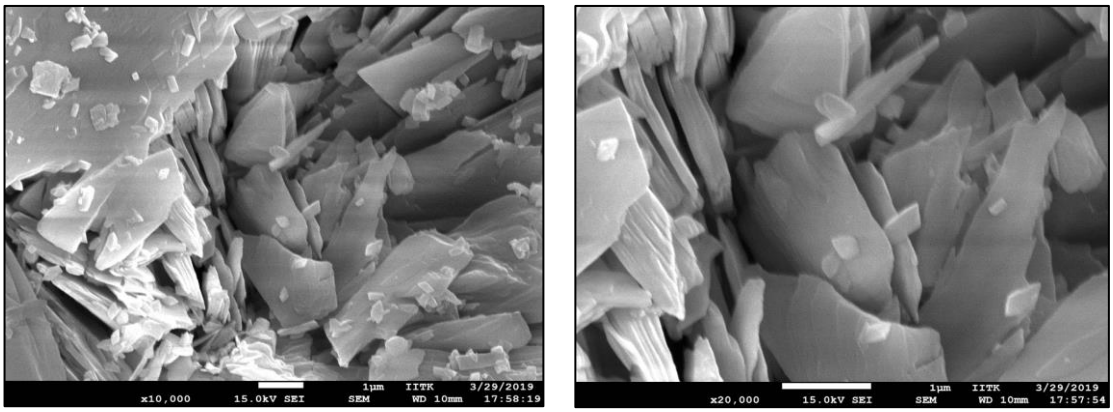

(a) (b)

Figure 2. (a-b) SEM micrographs of the parchment-supported barium molybdate membrane

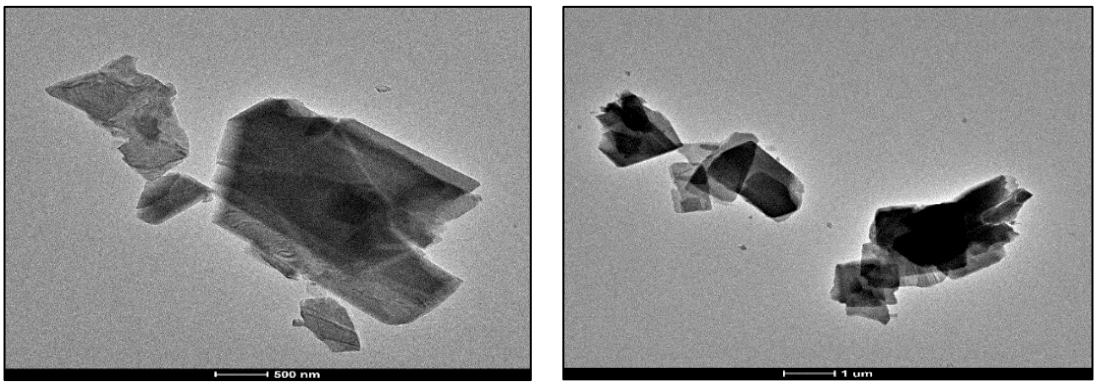

(a) (b)

Figure 3. (a-b) TEM images of the parchment-supported barium molybdate membrane

SEM micrographs of the parchment-supported barium molybdate membrane are shown in Figure 2. SEM images shows porosity, deviations and breakages or cracks on the surface of the membrane. Particles in the prepared membrane are irregularly condensed and adopt a heterogeneous structure composed of masses of different sizes.

The TEM images of the barium molybdate parchment-supported membrane are shown in Figure 3. It can be seen that the barium molybdate particles are reliably distributed on the surface of parchment paper, which means they are homogeneously distributed throughout the membrane. It is also clear from the micrographs that the binder has very good binding properties with inorganic molybdate.

FT-IR spectroscopy was used to study the structural characterization and bonds of the membrane material. Figure 4 indicates the FT-IR spectrum of the parchment-supported barium molybdate membrane. A strong absorption peak at 3678.170 cm^{-1} clearly indicates the presence of H_2O molecules. The weak absorption peaks in the range of 2368.49 cm^{-1}, 1676.07 cm^{-1}, 1573.85 cm^{-1} and 887.22 cm^{-1} indicate the presence of C-H bond, -O-H bending vibration, M-X bond and Mo=O bond of the model membrane respectively.

The TGA/DTA curve of the parchment-supported membrane is shown in Figure 5. The TGA curve of barium molybdate indicates the weight loss at different temperatures up to 600°C . The first weight loss of 14.95 mg at 277.36°C and second weight loss of 14.51 mg at 324.59°C were due to the parchment-supported material. So, it is clear that there was gradual weight loss on increasing the temperature. Therefore, it is obvious that the material has a hydrophilic nature that could absorb moisture from the surrounding atmosphere.

There is also a DTA curve showing a temperature reduction at 217.26 and 271.04°C. Therefore this material has an endothermic nature.

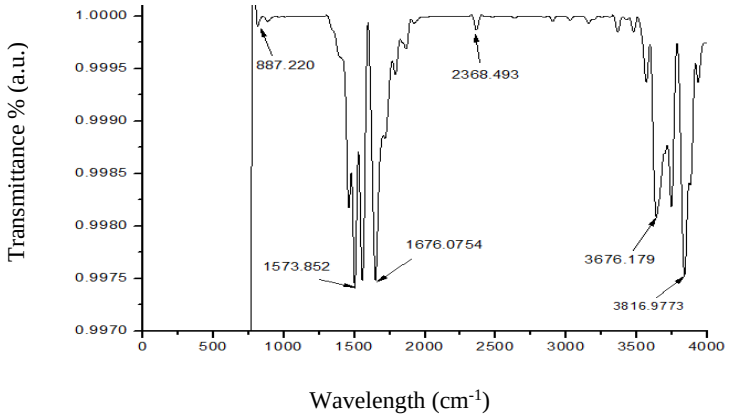

Figure 4. FT-IR Spectrum of the parchment-supported barium molybdate membrane

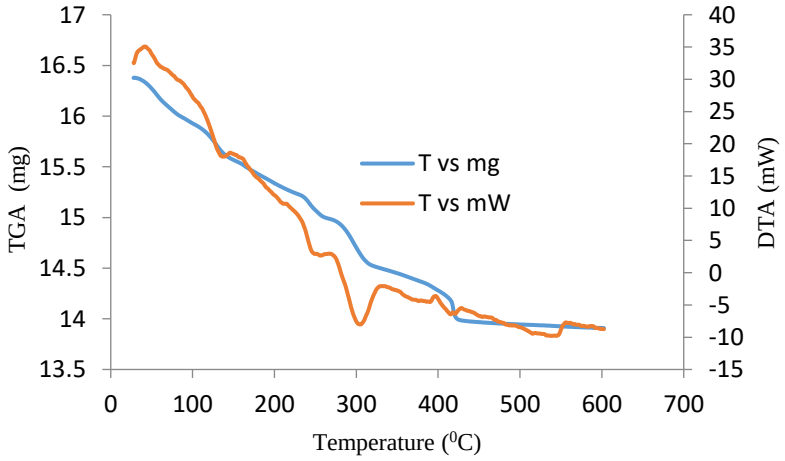

Figure 5. TGA/DTA curve of parchment-supported barium molybdate membrane

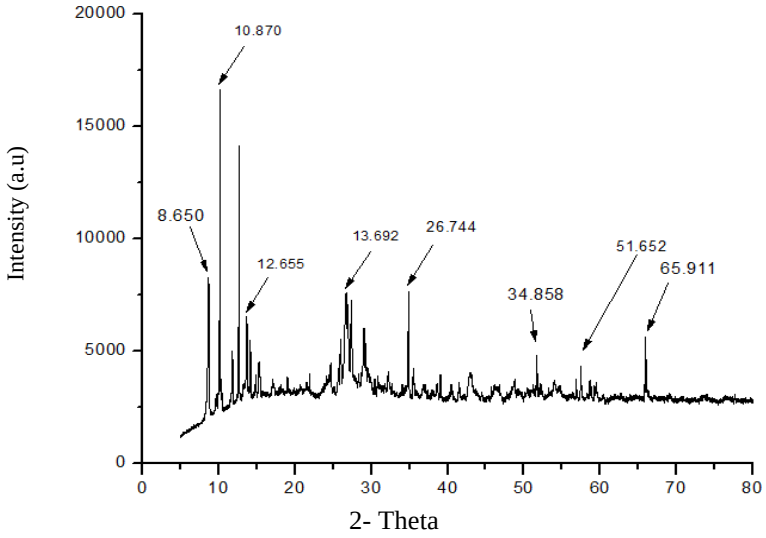

Figure 6. XRD spectra of parchment-supported barium molybdate membrane

The XRD spectrum of the membrane is shown in Figure 6. This spectrum shows sharp peaks of different intensities at different values of 2-Theta. All strong (8.650, 10.870 and 12.655) and weak (34.858, 51.652 and 65.911) peaks are found in the range of 10-80˚, which corresponds to some planes at different ranges. This analysis indicated that the parchment-supported barium molybdate membrane has a crystalline nature.

The EDX spectrum of the membrane is shown in Figure 7 and the overall results of the analysis of synthesized membrane particles in this study are given in Table 2. The presence of chemical constituents (Mo, O, C, Ba, Na, and Ti) in the EDX spectrum in their respective ratios confirms the formation of a parchment-supported barium molybdate model membrane.

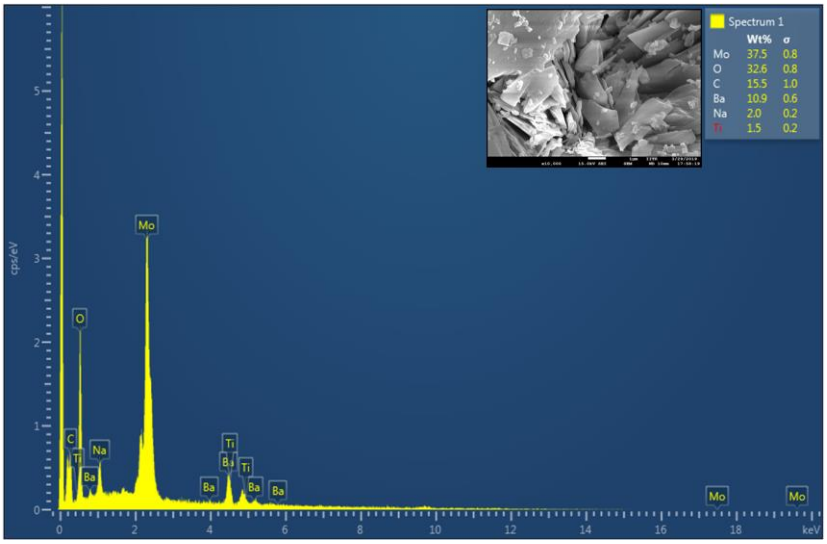

Figure 7. SEM supported EDX spectrum of the barium molybdate membrane

Table 2. Elemental analysis of the parchment-supported barium molybdate membrane particle

Element	% Wt.	σ (error)
Molybdenum	37.5	0.8
Oxygen	32.6	0.8
Carbon	15.5	1.0
Barium	10.9	0.6
Sodium	2.0	0.2
Titanium	1.5	0.2

The antibacterial activity of the parchment-supported barium molybdate membrane was tested under *in vitro* conditions against two Gram-negative bacteria, *Escherichia coli* (K 12) and *Pseudomonas aeruginosa* (MTCC 2488), and one Gram-positive bacteria, *Staphylococcus aureus* (MSSA 22), using the disc diffusion method. Different drugs like Cefotaxime, Augmentin, Chloramphenicol, ofloxacin, Co-Trimoxazole, Ciprofloxacin, Erythromycin, Gentamicin, Lincomycin, Penicillin G and Vancomycin were used as standards for the comparison of results. The results for erythromycin are given in Table 3.

Erythromycin (with concentrations of 10, 10 and 15 µg/disc, HiMedia) was less sensitive against the two Gram-negative and one Gram-positive bacteria (with zones of inhibition of 13, 13 and 16 millimeters) respectively. It was observed that the synthesized barium molybdate membrane had extraordinary inhibitory effects against the growth of bacteria.

The barium molybdate membrane had the highest inhibition against Gram-positive bacteria in comparison to Gram-negative bacteria and the control as shown in Table 3. Tetrahydrofuran (THF) as a control did not show a clear zone of inhibition of bacterial growth in any plate as shown in Figure 8. Therefore, it is clear that the model membrane can be used as a potent antibacterial agent.

Table 3. Antibacterial activity of parchment-supported barium molybdate membrane (with zone of inhibition in mm)

Bacteria	Barium molybdate membrane	THF (as control)	Erythromycin (as standard antibiotic)
Escherichia coli	13	13	5
Pseudomonas aeruginosa	13	14	7
Staphylococcus aureus	16	6	7

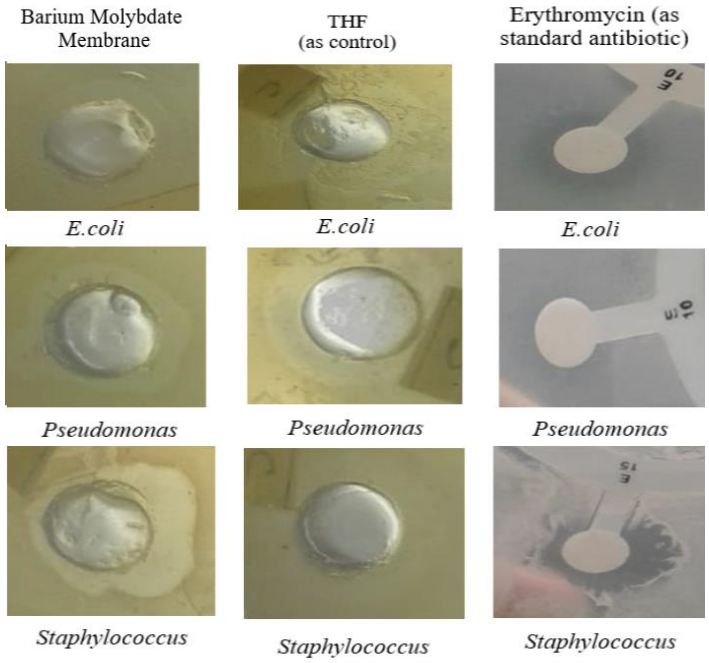

Figure 8. Diameter of zone of inhibition of parchment-supported barium molybdate membrane, THF (as control) and erythromycin (as standard antibiotic)

$$\Delta\psi = 59.2 \left[\log \frac{C_2 \left(4C_1^2 + \overline{X}^2\right)^{1/2} + \overline{X}}{C_1 \left(4C_2^2 + \overline{X}^2\right)^{1/2} + \overline{X}} + \overline{U} \log \frac{\left(4C_2^2 + \overline{X}^2\right)^{1/2} + \overline{X}\ \overline{U}}{\left(4C_1^2 + \overline{X}^2\right)^{1/2} + \overline{X}\ \overline{U}} \right] \quad (1)$$

Membrane theories:

Fixed Charge Theory of Teorell-Meyer and Seviers (TMS)

In the Teorell-Meyer and Seviers theory there must be an equilibrium process at each salt solution membrane interface which has a suitable analogy with the Donnan equilibrium.

According to the Teorell-Meyer and Seviers theory, the membrane potential applicable to a highly idealized system is proposed by the following equation (1) at 25°C:

where $\overline{U} = (\overline{u} - \overline{v})/(\overline{u} + \overline{v})$

$\overline{u}$ and $\overline{v}$ are the ionic mobilities of cation and anion (m^2/v/s) respectively within the membrane, C_1 and C_2 are the concentrations of the 1:1 electrolytic solutions on either side of the model membrane and $\overline{X}$ is the charge density (eq/l) on the membrane. The plotting method of Teorell-Meyer and Seviers determines the fixed charge density $\overline{X}$ and the cation-to-anion mobility ratio in the membrane phase.

Fixed Charge Theory of Kobatake and Nagasawa

Kobatake et.al [28, 29] and Nagasawa et.al [30, 31] have been accepted to evaluate the charge density of a membrane of uniform thickness which separates two bulk solutions of various uni-univalent electrolyte concentrations C_1 and C_2. The membrane potential with salt concentrations is proposed by Nagasawa in equation (2).

Here, $\overline{X}$ denotes the effective fixed charge density of charged membrane.

Kobatake et.al. developed the expression for membrane potential as described in equation (3)

Here, K denotes a constant dependent upon the viscosity of the salt solution and structural details of the polymer network of which material the membrane is composed. Membrane parameters α, β and $\overline{X}$ have been assumed to be independent of the electrolyte concentration.

Kobatake has derived two useful limiting forms of equation (3). When C_2 becomes sufficiently small with γ fixed, the equation can be expanded to give in equation (4).

Where $\sigma_{\Delta\psi}$ is the absolute value of a reduced membrane potential given by in equation (5).

Kobatake has also shown that at a fixed γ the inverse of an apparent transference number t_{-app} for the co-ion species in a charged membrane is proportional to the inverse of the concentration C_2 at high salt concentration. Apparent transference number is defined by the relation - equation (6).

$$-\Delta\psi = \frac{RT}{F}\left(\frac{\gamma}{\gamma - 1}\right)\left(\frac{\overline{X}}{2}\right)\frac{1}{C_2} \quad (2)$$

$$\Delta\psi = -\frac{RT}{F}\left[\frac{1}{\beta} \ln \frac{C_2}{C_1} - \left(1 + \frac{1}{\beta} - 2\alpha\right) x \ln\left(\frac{C_2 + \alpha\beta\overline{X}}{C_1 + \alpha\beta\overline{X}}\right)\right] \quad (3)$$

where

$$\alpha = u/(u+v)$$

$$\beta = 1 + \left(\frac{KF\overline{X}}{u}\right)$$

$$\sigma_{\Delta\psi} = \frac{1}{\beta} \ln \gamma - \left(\frac{\gamma - 1}{\alpha\beta\gamma}\right)\left(1 + \frac{1}{\beta} - 2\alpha\right)\left(\frac{C_2}{\overline{X}}\right) \quad (4)$$

$$\sigma_{\Delta\psi} = F\Delta\psi / RT \quad (5)$$

and $\gamma = C_2 / C_1$

$$\frac{1}{t_{-app}} = \frac{1}{1-\alpha} + \frac{(1+\beta-2\alpha\beta)(\gamma-1)\alpha}{2(1-\alpha)^2 \ln \gamma}\left(\frac{\bar{X}}{C_2}\right)+.... \quad (6)$$

Table 4. Experimentally observed membrane potential (mV) values across the parchment-supported barium molybdate membrane in contact with different uni-univalent electrolytes at 25±0.1°C

Concentration (mol/l)	Electrolytes		
	KCl	NaCl	LiCl
1.0/0.1	10.6	12.4	14.9
0.5/0.05	15.1	17.2	19.7
0.1/0.01	22.2	24.5	26.9
0.05/0.005	32.1	34.2	36.8
0.01/0.001	41.9	44.1	46.9
0.005/0.0005	49.2	51.1	54.1

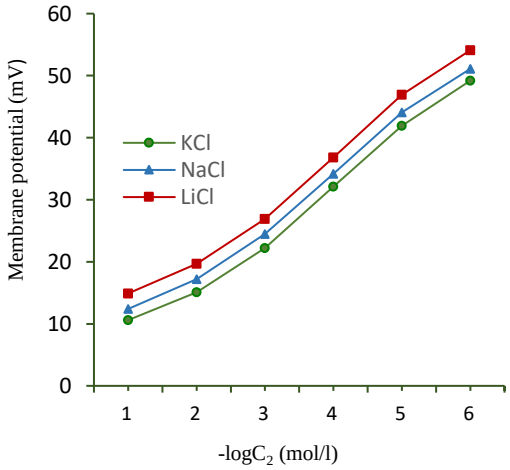

Figure 9. Plots of membrane potential (mV) against -logC_2 using uni-univalent electrolytes across the barium molybdate parchment-supported model membrane

Here, α is the molar mobility ratio of cation to the adding of molar mobilities of cation and anion, C_2 (in mol/dm^2) is the uni-univalent electrolyte concentration in the lower concentration side of the cell and $\bar{X}$ denotes the charge density of the fabricated membrane under investigation.

The membrane potential values measured across the barium molybdate parchment-supported model membrane in contact with different uni-univalent electrolytes at 25 ± 0.l °C are given in Table 4 and plotted against -logC_2 as shown in Figure 9.

The theoretical membrane potentials for a cation-selective membrane is calculated from equation (1). These curves appear in Figure 10. The difference curves are for different mobility ratios ($\bar{u}/\bar{v}$), with a uniform value of $\bar{X}$ expressed in equivalents/litre. The experimentally-observed membrane potential values for the barium molybdate membrane with KCl salt were plotted in an identical graph against a function of -logC_2. The experimental curve was moved horizontally and ran parallel to one of the theoretical curves. The calculated data of effective fixed charge density $\bar{X}$ obtained in this way for the model membrane and uni-univalent electrolytes are given in Table 5.

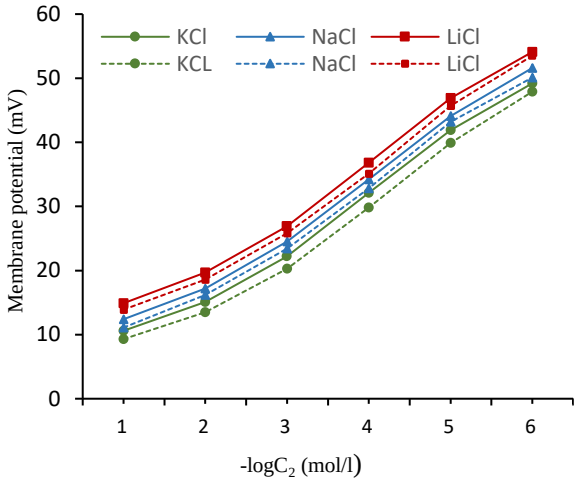

Figure 10. Plot of membrane potential against -logC_2 for the barium molybdate parchment-supported membrane. The smooth curves are the theoretical concentration potentials for different mobility ratios. The solid line consists of the experimental membrane potential values of the for different concentrations of KCl solution

Table 5. Comparison of the values of the effective fixed charge density calculated from different methods of the parchment-supported barium molybdate membrane in contact with various uni-univalent electrolytic solutions

Electrolytes	TMS Method $\overline{X} \times 10^2$ [equation 1]@	Nagasawa Method $\overline{X} \times 10^2$ [equation 2]©	Kobatake Method $\overline{X} \times 10^2$ [equation 6]®
KCl	0.98	1.22	3.99
NaCl	1.10	1.27	4.12
LiCl	1.31	1.41	5.22
	@ with the slop of Figure 10	© with the slop of Figure 11	®with the slop of Figure 13

Equation (2) represents the plot of $_{\Delta\psi}$ against $1/C_2$ which is linear as shown in Figure 11 with a slope equal to $\frac{RT}{F}\left(\frac{\gamma}{\gamma-1}\right)\left(\frac{\overline{X}}{2}\right)$ from which the data of $\overline{X}$ for different electrolytes have been evaluated. The calculated values of fixed charge density are given in Table 5.

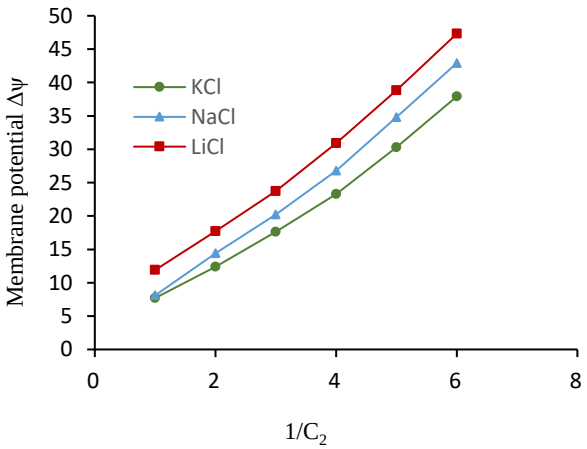

Figure 11. Potential values (mV) plotted against $1/C_2$ (dm^3 /mol) for the parchment-supported barium molybdate membrane with different salt solutions

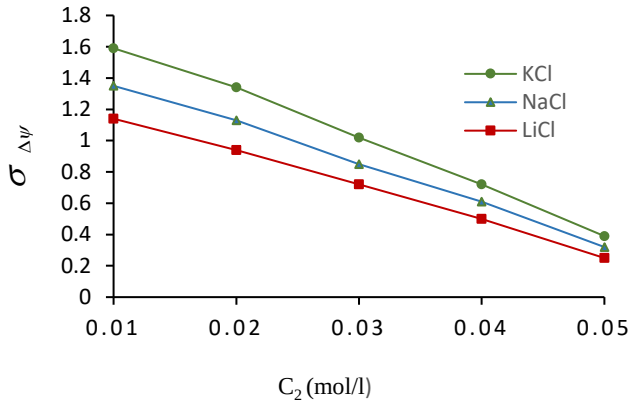

Figure 12. Plots of $\sigma_{\Delta\psi}$ against C_2 for the parchment-supported barium molybdate membrane using various uni-univalent electrolytes

Table 6. α and β values for the parchment-supported barium molybdate membrane-electrolyte system

Electrolytes	Barium molybdate membrane	
	α	β
KCl	0.45	1.59
NaCl	0.41	2.20
LiCl	0.40	2.11

Equation (4) indicates that the β value and a relation between α and $\overline{X}$ can be obtained by evaluation of the intercept and the initial slope of a plot of $\sigma_{\Delta\psi}$ against C_2 which is shown in Figure 12. The value of the intercept is equal to $\frac{1}{\beta}\ln\gamma$ from which β is evaluated. The values are given in Table 6.

Equation (6) indicates that α and $\overline{X}$ can be calculated from the intercept of a linear plot of $1/t_{-app}$ against $1/C_2$ for different uni-univalent electrolytes as shown in Figure 13. The intercept value is equal to $1/(1-\alpha)$, from which α may be evaluated. The values are given in Table 6. The calculated data of the fixed charge densities $\overline{X}$ for the barium molybdate membrane are also given in Table 5. The fixed charge densities of the model membrane under different salt environments were found to follow the order: LiCl > NaCl > KCl.

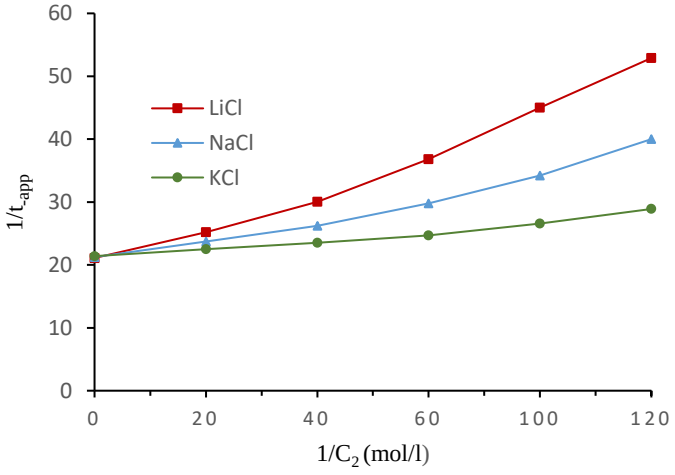

Figure 13. Plots of $1/t_{-app}$ against l/C_2 (dm^3/mol) for the parchment-supported barium molybdate membrane with various electrolytes

$$\Delta\psi = \Delta\psi_{Donn} + \Delta\psi_{Diff} \tag{7}$$

$$\Delta\psi = -\frac{RT}{V_K F}\ln\left(\frac{\gamma_{2\pm} C_2 \overline{C}_{1+}}{\gamma_{1\pm} C_1 \overline{C}_{2+}}\right) - \frac{RT\overline{\omega}-1}{V_K F\overline{\omega}+1}\times\ln\left(\frac{(\overline{\omega}+1)\overline{C}_{2+} + \left(V_X/V_K\right)\overline{X}}{(\overline{\omega}+1)\overline{C}_{1+} + \left(V_X/V_K\right)\overline{X}}\right) \tag{8}$$

$$C_+ = \sqrt{\left(\frac{V_X\overline{X}}{2V_K}\right)^2\left(\frac{\gamma_\pm C}{q}\right)^2} - \frac{V_X\overline{X}}{2V_K} \tag{9}$$

$$q = \sqrt{\frac{\gamma_\pm}{K_\pm}} \tag{10}$$

$$K_\pm = \frac{\overline{C}_i}{C_i}, \qquad \overline{C}_i = C_i - \overline{D} \tag{11}$$

$$\Delta\psi = \frac{RT}{F}(t_+ - t_-)\ln\frac{C_2}{C_1} \tag{12}$$

where

$$\frac{t_+}{t_-} = \frac{\overline{u}}{\overline{v}} \tag{13}$$

The Teorell-Meyer-Sievers equation (1) can also be expressed by the adding of a Donnan potential $\Delta\psi_{Donn}$ between membrane surfaces and external solutions and therefore the diffusion potential $\Delta\psi_{Diff}$ within the model membrane as shown in equation (7) to equation (8) [32, 33].

The R, T and F have their significance values, $\gamma_{1\pm}$ and $\gamma_{2\pm}$ are mean ionic activity coefficients, $\overline{\omega} = \overline{u}/\overline{v}$ represents the mobility ratio of the fabricated membrane and C_{1+}, C_{2+} are the cation concentration in both side of charged membrane. Here V_k and V_x represented the valency of cations and fixed-charge group on the membrane matrix. The cation concentration is given by the equation (9).

where q denotes the charge effectiveness of the fabricated membrane and is defined by the following equation (10).

Here $K_\pm$ is the distribution coefficient which is expressed in equation (11).

where $\overline{C}_i$ denotes the i^{th} ion concentration within the membrane phase and Ci denotes the i^{th} ion concentration of the external solution. The transport properties of the membrane in various salt solutions are important parameters to further investigate the membrane phenomena as shown in equation (12).

Equations (12) and (13) have been used to get the transference numbers t_+ and t- values from the observed membrane potential data. The values of t_+ are given in Table 7. The mobility values were calculated using the transference number. The mobility ratio $\overline{\omega} = \overline{u}/\overline{v}$ and $\overline{X}$ are given in Table 7. The values of the mobility ratio $\overline{\omega}$ of different salts in the membrane phase were found to be higher at lower concentrations of all uni-univalent salts. Further, higher concentrations of different salts led to a sharp drop in the mobility ratio $\overline{\omega}$ values as seen in Figure 14. The higher mobility is attributed to a higher transference number of comparatively free cations of salts as shown in Figure 15 and also follows similar trends in lower concentration salt solutions. The data of the various membrane parameters $K_\pm$, q and C_+ derived for the system have also been calculated in Table 8. Using equation (11) it was found that the distribution coefficient values increased at lower salt solution concentrations. As the salt concentration increased, the distribution coefficient values sharply decreased, and thereafter, a stable trend was determined as can be seen in Table 8 and Figure 16.

Table 7. The calculated data of the t_+, $\overline{X}$ and $\overline{\omega}$ parameters of the parchment-supported barium molybdate membrane using different uni-univalent salt solutions

Concentration (mol/l)	Parameters		
	t_+	$\overline{X}$	$\overline{\omega}$
KCl			
0.005	0.82	0.61	4.71
0.01	0.79	0.59	4.21
0.05	0.68	0.42	2.41
0.1	0.53	0.13	1.59
0.5	0.52	0.12	1.38
1.0	0.51	0.10	1.29
NaCl			
0.005	0.76	0.52	3.12
0.01	0.74	0.33	3.10
0.05	0.62	0.23	2.12
0.1	0.54	0.16	1.45
0.5	0.53	0.10	1.30
1.0	0.51	0.09	1.21
LiCl			
0.005	0.78	0.49	3.00
0.01	0.71	0.47	2.90
0.05	0.63	0.36	2.01
0.1	0.56	0.31	1.31
0.5	0.54	0.11	1.20
1.0	0.52	0.05	1.17

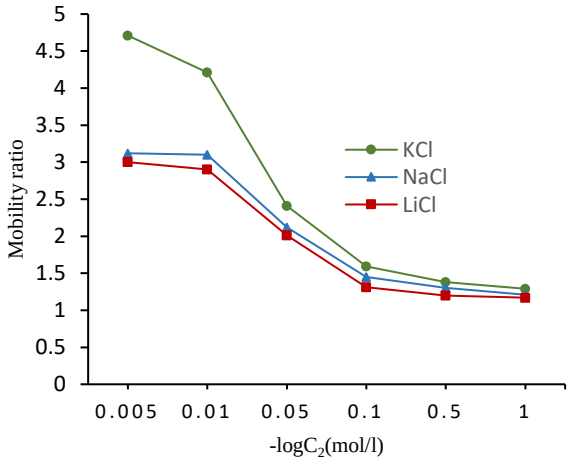

Figure 14. Plots of mobility ratio against -logC_2 of the barium molybdate membrane with uni-univalent electrolytes

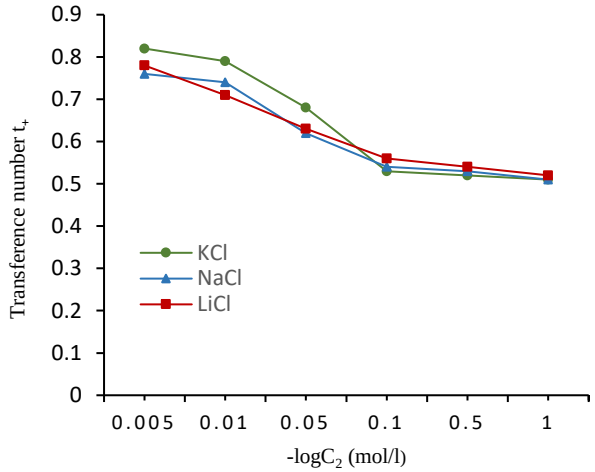

Figure 15. Plots of t_+ (transference number) against -logC_2 of the barium molybdate membrane using uni-univalent electrolytes

Table 8. The calculated data of the parameters $K_{\pm}$, q and C_+ of the parchment-supported barium molybdate membrane with different uni-univalent salt solutions

Concentration (mol/l)	Parameters		
	$K_{\pm}$	q	C_+
KCl			
0.005	4.61	0.56	0.0028
0.01	4.21	0.62	0.0026
0.05	0.03	5.59	0.0059
0.1	0.52	1.58	0.0422
0.5	1.10	0.86	0.0521
1.0	1.45	0.82	0.6910
NaCl			
0.005	3.10	0.59	0.0019
0.01	2.51	0.63	0.0017
0.05	0.37	1.69	0.0064
0.1	0.71	1.02	0.0423
0.5	0.83	0.99	0.0399
1.0	0.99	0.81	0.6221
LiCl			
0.005	2.98	0.56	0.0018
0.01	2.12	0.50	0.0017
0.05	0.46	1.57	0.0088
0.1	0.90	1.03	0.0392
0.5	0.69	1.01	0.0310
1.0	0.85	0.81	0.7012

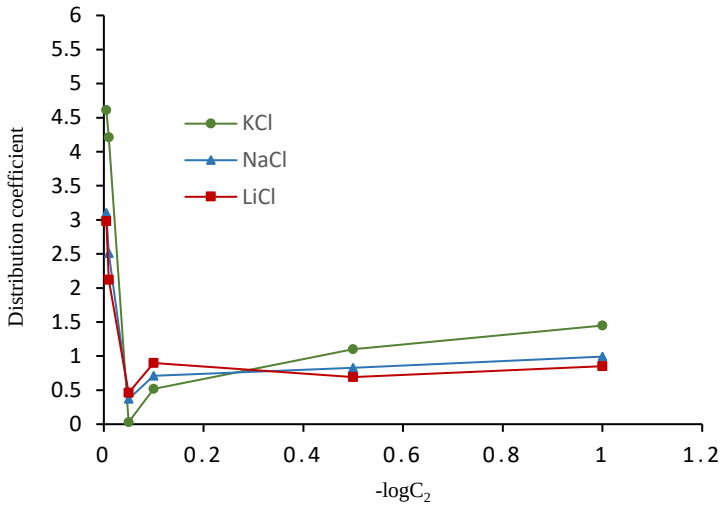

Figure 16. Plots of distribution coefficients against -logC_2 for the parchment-supported barium molybdate membrane with different uni-univalent electrolytes

Ion selectivity of the model membrane also can be expressed as a function of permselectivity, Ps which is defined as a measure of preferential permeation of counter-ions inside the membrane instead of the solution (outside the membrane). Applying methods proposed by HelfFerich [34], permselectivity has been calculated by the following equation:

$$Ps = \left(\frac{t_+^m - t_+}{1 - t_+} \right) \qquad (14)$$

Permselectivity is often calculated using equation (14). It can be seen from Figure 17 that permslectivity decreased with the increase in concentration of the electrolyte solution. This does not conform with the expectation that increased deswelling of the prepared membrane results in progressively lowered co-ion exclusion with an increase in electrolyte concentration.

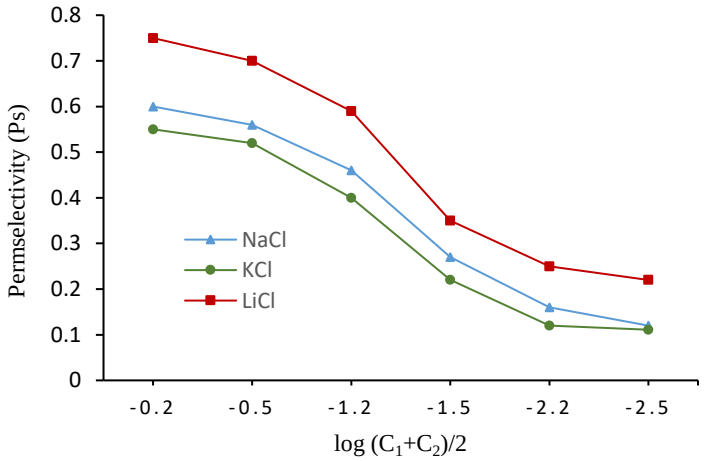

Figure 17. Plots of Ps against log (C_1+C_2)/2 for the parchment-supported barium molybdate membrane with different uni-univalent electrolytes

CONCLUSION

The membrane potential of a newly-prepared barium molybdate membrane was measured with uni-univalent salt (chlorides of potassium, sodium and lithium) solutions using standard electrodes. The membrane potential values obtained by different electrolytes followed the order: LiCl > NaCl > KCl and the obtained data indicates that the behavior of the investigated membrane is cation-selective for lithium ions. The charge density value is highest for lithium ions in all the theories as the Donnan exclusion is maximum for a salt of smaller cation size. The permselectivity and effective fixed charge density values were found to be in the following order: LiCl > NaCl > KCl for the same electrolyte concentrations. Moreover, the fixed charge density values evaluated by other approaches were found to be in close agreement. The antibacterial activity study revealed that the membrane shows good antibacterial activity. The scope of this membrane has great potential for use in desalination and industrial applications.

ACKNOWLEDGEMENT

The authors gratefully acknowledge the principal of S.M.S. Govt. Model Science College, Gwalior-474009, Madhya Pradesh for providing the necessary research facilities.

REFERENCES

1. Matsumoto, H., Chen, Y. C., Yamamoto, R., Konosu, Y., Minagawa, M., Tanioka, A. (2005) Membrane potentials across nanofiltration membranes: effect of nanoscaled cavity structure. *J. Mol. Struct*., **739**, 99–104.

2. Weqar, S., Khan, A., Shakeel, A., Inamuddin (2007) Synthesis, characterization and ionexchange properties of a new and novel 'organic–inorganic' hybrid cationexchanger: Poly(methyl methacrylate) Zr(IV) phosphate. *Colloid. Surf*, **295**, 193–199.

3. Chou, T. J., Tanioka, A. (1998) Ionic behavior across charged membranes in methanol water solutions. I: Membrane potential. *J. Membr. Sci*., **144**, 275–284.

4. Khan, M. M. A., Kumar Manoj (2018) Electrochemical Properties and Antibacterial Activity of Polyvinyl Chloride Supported Silver Molybdate Ion-Exchange Composite Membrane. *Journal of Membrane Science and Research*, **4**, 15–19.

5. Anastasova, S., Radu, A., Matzeu, G., Zuliani, C., Mattinen, U., Bobacka, J., Diamond, D. (2012) Disposable solid-contact ion-selective electrodes for environmental monitoring of lead with ppb limit-of-detection. *Electrochim. Acta*, **73**, 93–97.

6. Guzin´ ski, M., Lisak, G., Kupis, J., Jasin´ ski, A., Bochen´ ska, M. (2013) Lead (II)-selective ionophores for ion-selective electrodes: A review. *Anal. Chim. Acta*, **791**, 1–12.

7. William D. Mulhearn, Vladimir P. Oleshko, Christopher M. Stafford (2021) Thickness-dependent permeance of molecular layer-by-layer polyamide membranes. *Journal of membrane science*, **618**, 118637.

8. Inamuddin, Mu. Naushad, Tauseef Ahmad Rangreez, ALOthman Z. A. (2015) Ion-selective potentiometric determination of Pb(II) ions using PVC-based carboxymethyl cellulose Sn(IV) phosphate composite membrane electrode. *Desalination and Water Treatment*, **56**, 806–813.

9. Siddiqi, F. A., Beg, M. N., Singh, S. P. (1979) Studies with model membranes. X. Evaluation of the thermodynamically effective fixed charge density and perm selectivity of mercuric and cupric iodide parchment-supported membranes. *J. Poly. Sci*., **15**, 959–972.

10. Arsalan, M., Rafiuddin (2014) Binding nature of polystyrene and PVC 50:50% with CP and NP 50:50% ion exchangeable, mechanically and thermally stable membrane. *J. Ind. Eng. Chem*., **20**, 3283–3291.

11. Ishrat, U., Rafiuddin (2012) Synthesis, characterization and electrical properties of Titanium molybdate composite membrane Desalination**, 286**, 8–15

12. Hao Pingjiao, Wijmans, J. G. (2020) Effect of pore location and pore size of the support membrane on the permeance of composite membranes, **594**, 117465.

13. Elsherif, K. M., Yaghi, M. M. (2017) Membrane Potential Studies of Parchment Supported Silver Oxalate membrane. *JMES*, **1(8)**, 117465.

14. Matsumoto, H., Konosu, Y., Kimura, N., Minagawa, M., Tanioka, A. (2007) Membrane potential across reverse osmosis membranes under pressure gradient. *J. Colloid Interface Sci.*, **272**, 309.

15. Imteyaz Shahla, Rafiuddin (2016) Transport studies of ions across polystyrene based composite membrane: Evaluation of fixed charge density using theoretical models Journal of Molecular Structure, 1-18.

16. Sumit S. Bhattad, Prakash A. Mahanwar (2019)

Preparation and Physical Characterization of Sulfonated Poly (Ether Ether Ketone) and Polypyrrole Composite Membrane. *Journal of Membrane Science and Research*, **5**, 49–54.

17. Melike Begum Tanis-Kanbur, René I. Peinador, José I. Calvo, Antonio Hernández, Jia Wei Chew (2021) Porosimetric membrane characterization techniques: A review. *Journal of Membrane Science*, **619**, 118750.

18. Tengku Sallehuddin, T. N. A., Abu Seman, M. N. (2017) Modification of Thin Film Composite Nanofiltration Membrane using Silver Nanoparticles: Preparation, Characterization and Antibacterial Performance. *Journal of Membrane Science and Research*, **3**, 29–35.

19. Beg, M. N., Siddiqi, F. A. and Shyam, R. (1977) Studies with inorganic precipitate membranes: part XIV. Evaluation of effective fixed charge densities. *Can J. Chem.*, **55**, 1680–1686.

20. Beg, M. N., Siddiqi, F. A., Shyam, R. and Altaf, I. (1978) Studies with inorganic precipitative membranes: XI. Membrane potential response, characterization and evaluation of effective fixed charge density. *J. Electroanal Chem. Interfacial Electrochem*, **89**, 141–147.

21. Beg, M. N., Siddiqi, F. A., Singh, S. P., Prakash, P. and Gupta, V. (1979) Studies with inorganic precipitate membrane: evolution of thermodynamically effective fixed charge density and test of the most recently developed theory of membrane potential based on the principles of non-equilibrium thermodynamics. *Electrochim Acta*, **24**, 85–88.

22. Beg, M. N. and Matin, M. A. (2002) Studies with nickel phosphate membranes: evaluation of charge density and test of recently developed theory of membrane potential. *J. Memb. Sci*., **196**, 95–102.

23. Kushwaha, R. S., Ansari Mohd. Ayub, Singh Neelam, Kumar Manoj and Beg, M. N. (2010) Synthesis of poly-styrene based nickel phosphate membranes and evaluation of membrane parameters to test the membrane potential theories. *J. Ind. Chem. Soc.*, **87(4)**, 471–479.

24. Arsalan, M., Rafiuddin (2014) Fabrication, characterization, transportation of ions and antibacterial potential of polystyrene based Cu3 (PO4)2/Ni3 (PO4)2 composite membrane. *J. Ind. Eng. Chem*., **20**, 3568–3577.

25. Matin, M. M., Bhattacharjee, S. C., Chakraborty, P. and Alam, M. S. (2019) Synthesis, PASS predication, in vitro antimicrobial evaluation and pharmacokinetic study of novel n-octyl glucopyranoside esters. *Carbohydrate Research*, **485**, 107812.

26. Matin, M. M., Chakraborty, P., Alam, M. S., Islam, M. M. and Hanee, U. (2020) Novel mannopyranoside esters as sterol 14α-demethylase inhibitors: Synthesis, PASS predication, molecular docking, and pharmacokinetic studies. *Carbohydrate Research*, **496**, 108130.

27. Arsalan Mohd., Zehra Aiman, Khan Mohammad Mujahid Ali (2019) Preparation and characterization of Polyvinyl chloride based nickel phosphate ion selective membrane and its application for removal of ions through water bodies. *Groundwater for Sustainable Development*, **8**, 41–48.

28. Kobatake, Y. (1958) Irreversible Electrochemical Processes of Membranes. *J. Chem. Phys*., **28**, 146–153

29. Toyoshima, Y., Kobatake, Y., Fujita H. (1967) Studies of membrane potential. Part 4. Membrane potential and permeability. *Trans. Faraday Soc.*, **63**, 2814–2827.

30. Tasaka, M., Nagasawa, M. (1978) Thermoosmosis through charged membranes theoretical analysis of concentration dependence. *Biophysical chemistry*, **8(2)**, 111–116.

31. Nagasawa, M., Kobatake, Y. (1952) The Theory of Membrane Potential. *J. Phys. Chem*., **56**, 1017–1024.

32. Matsumoto, H., Tanioka, A., Murata, T. J., Higa, M., Horiuchi, K. (1998) Effect of proton on potassium ion in counter transport across fine porous charged membranes. *J. Phys. Chem. B.*, **102**, 5011.

33. Chou, T. J., Tanioka, A. (1999) Membrane Potential of Composite Bipolar Membrane in Ethanol–Water Solutions: The Role of the Membrane Interface. *J. Colloid Interface Sci*., **212**, 293.

34. Helfferich, F.G. (1962) Ion Exchange, Dover Publication, New York.